

Review Article

Optical Emission of the Nuclear-Induced Plasmas of Gas Mixtures

Mendykhan U. Khasenov

Nazarbayev University Research and Innovation System PI, Astana 010000, Kazakhstan

Correspondence should be addressed to Mendykhan U. Khasenov; mendykhan.khasenov@nu.edu.kz

Received 30 December 2013; Revised 24 March 2014; Accepted 24 March 2014; Published 27 April 2014

Academic Editor: Gong-Ru Lin

Copyright © 2014 Mendykhan U. Khasenov. This is an open access article distributed under the Creative Commons Attribution License, which permits unrestricted use, distribution, and reproduction in any medium, provided the original work is properly cited.

The characteristic properties of the inverted-population-forming processes in lasers with ionizing pumping are considered. Results obtained from research of active laser media concerning the p-s transitions of atoms of neon, mercury, and cadmium are presented. The feasibility of ion-ion recombination in lasers with nuclear pumping is discussed. The excitation kinetics of the first negative system of CO, heteronuclear ionic molecules of inert gases, and halogenides of inert gases under ionizing radiation are considered.

1. Introduction

The study of the optical (laser or spontaneous) radiation of nuclear-excited plasmas is of interest for the development of a method to extract energy from nuclear reactors and also to control and adjust the nuclear reactors' parameters. It is assumed that in the future, nuclear-pumped lasers will be used for a wide range of applications [1–3], especially in cases when powerful compact lasers must be placed at autonomous remote sites. The direct pumping of active laser media is generally achieved by means of products of nuclear reactions involving thermal neutrons from the nuclear reactor: ${}^3\text{He}(n,p){}^3\text{H}$, ${}^{10}\text{B}(n,\alpha){}^7\text{Li}$, ${}^{235}\text{U}(n,f)\text{F}$, and others. Such active laser media containing ${}^{235}\text{U}$, ${}^3\text{He}$, or ${}^{10}\text{B}$ or compounds that contain these isotopes are applied to the walls of the laser chamber. There is also substantial research interest in this field related to the difference between the level-population mechanisms under nuclear pumping and the population processes in a common gas-discharge laser. Current lasers with nuclear pumping [2] radiate in the spectral band of 391–5600 nm, at approximately 50 transitions of Xe, Ar, Kr, Ne, C, N, Cl, O, I, and Hg atoms, Cd^+ , Zn^+ , and Hg^+ ions, CO molecules, and N_2^+ molecular ions. Lasers with nuclear pumping at the xenon atomic transitions have been explored most thoroughly, and record-breaking pulsed power values of 1.3 MW and pulse energies of 520 joules have been achieved for lasers with nuclear pumping [4].

In this work, the experimental research efforts concerning the optical radiation of nuclear-induced plasmas performed at the Kazakhstan Institute of Nuclear Physics (INP) are analysed. In contrast with the majority of the scientific community, who have conducted their research regarding direct nuclear-pumped lasers by using pulse nuclear reactors with high neutron fluxes [1, 2], the research at the INP has been conducted using the stationary nuclear WWR-K reactor, which can produce thermal neutron fluxes up to 10^{14} n/cm²s. In this regime, the power density of the nuclear-reaction products that are transformed into gas does not exceed a few W/cm³, necessitating a search for active media with very low lasing thresholds. The advantage of experiments conducted using stationary nuclear reactors lies in the possibility to perform more detailed research concerning nuclear-induced plasma [5].

At INP, the study of lasers with direct nuclear pumping began in 1980 after the appearance of several publications regarding the creation of low-threshold lasers: these publications concerned an Ar-Xe mixture with a lasing threshold of $8 \cdot 10^{12}$ n/cm²s [6] and continuous helium-neon lasers at neutron fluxes of $2 \cdot 10^{11}$ n/cm²s [7]. According to the most optimistic forecasts, the power of the gas mixtures used for pumping (nuclear-reaction products from both ${}^3\text{He}$ and uranium fission fragments were used) in our experiments was sufficient to achieve laser action at the infrared transitions of

xenon. However, under the extreme conditions of a stationary nuclear reactor core (sound uniformity of temperature, high temperature, sputtering, and precipitation of impurities from the layer containing uranium), this proved to be insufficient [8]. The work of Carter et al., which was also performed using a stationary nuclear reactor, is worthy of special note. In our experiments, the neutron flux density was smoothly varying from 10^{11} to 10^{14} n/cm²s, but the lasing threshold in the ³He-Ne mixture was not reached [5, 8]. Moreover, in mixtures containing neon under ionizing pumping, emission at $\lambda = 632.8$ nm is nearly absent [9, 10]. The negative results of these early experiments revealed the necessity of searching for novel active media and novel schemes of level population, taking into account the characteristic properties of nuclear pumping.

2. Characteristic Properties of Processes in Lasers with Ionizing Pumping

In a quantum system, the gain (absorption) coefficient of a medium is described by the following expression [11]:

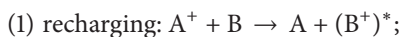
$$\alpha = \sigma \left(N_2 - N_1 \frac{g_2}{g_1} \right). \quad (1)$$

Here, the indices 1 and 2 refer to the upper level (2) and the lower level (1), N is the level population, and g is the statistical weight of the level. The cross-section of stimulated transition is calculated as follows:

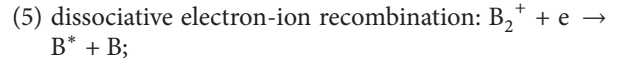
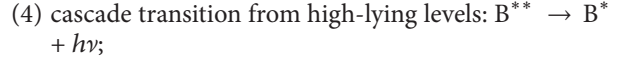
$$\sigma = \frac{\lambda^2}{2\pi} \frac{A}{\Delta\omega}, \quad (2)$$

where λ is the transition wavelength, $\Delta\omega$ is the line width, and A is the transition probability. In an amplifying medium ($\alpha > 0$), it is necessary to maintain a state of population inversion: the population of the upper level must exceed the population of level one (with the appropriate correction for degeneracy multiplicity). Either a favourable upper level population or the deactivation of the lower level is essential for the creation of an inverted population. Inversion may be achieved not only by preferential population of the upper level but also by selective deactivation of the lower level.

Gas lasers are distinguished by a variety of pumping methods: they may be based on electrical discharge, chemical reactions, gas-dynamic excitation, optical pumping, or pumping by electron beams or nuclear-reaction products, among other methods. In the vast majority of gas lasers, population inversion is generated by electrical discharge. The fundamental distinctive feature of lasers that operate via pumping by nuclear-reaction products or electron beams compared with gas-discharge lasers is that the population in many active media is determined not by electron impact at the lower levels but in the process of plasma recombination ("from the top downward"). In the first stage, the energy transfer from the atoms and ions of the easier buffer gas A to the atoms (molecules) of gas B occurs through one of the following processes:



The upper laser level may be populated either in one of these processes or in subsequent processes of plasma relaxation:



In gas-discharge lasers of low pressure, the lower laser level is typically deactivated in optical transitions to the low-lying levels; in lasers with nuclear pumping at atmospheric pressure, such depopulation occurs through collisions with medium atoms or plasma electrons and through Penning reactions with additional gas particles. In excimer lasers, where the excimer molecule transitions to the lower divergence or loosely bound state through photon emission, there is no problem with lower-level depopulation.

The characteristics of laser radiation under pumping by hard ionizers depend on the power and duration of the energy deposition into the active medium but do not depend on the type of ionizer [3]. This means that the kinetics of the processes in the active media of lasers excited by electron beams and lasers excited through nuclear pumping will be the same. Experiments concerning beam pumping may be used to model the properties of active media for nuclear pumping. The results of research regarding lasers with nuclear pumping may be applied in implementations of electron or ion beams [12, 13]. There is some difference between these two pumping methods because of the possibility of obtaining short and powerful beams of electrons. In pulse nuclear reactors, the pulse duration is in the order of tens of microseconds or more, which is much longer than the spontaneous lifetime of the laser levels (usually tens of nanoseconds). An electron beam provides an energy-deposition power of several MW/cm³, whereas in pulse nuclear reactors, at maximum neutron fluxes of 10^{17} n/cm²s, the pumping power does not exceed 5 kW/cm³ [2]. Therefore, laser action under nuclear pumping has a continuous or quasicontinuous nature (i.e., the duration of the laser radiation pulses is much longer than the lifetime of the laser levels).

3. Development of Experimental Methods

Spectral analysis of the luminescence of gas mixtures is the primary method that is applied in research of nuclear-induced plasmas. Under radioisotope pumping, 18 sources with ²¹⁰Po placed on the surface of each cylinder, which had a diameter of 25 mm and a length of 70 mm, were installed in a stainless-steel chamber [14]. The maximum ranges of α particles with an energy of 5 MeV in helium, argon, and xenon under normal conditions are 183, 37, and 25 mm, respectively. The chamber was heated and outgassed to vacuum of $\sim 10^{-3}$ Pa prior to the installation of the sources. After the installation of the α sources, the chamber was pumped without heating

for 2-3 weeks until well-reproducible (variation of no more than 3–7% in intensity, depending on the gas) spectra of luminescence were achieved. The gas pressure was monitored using a vacuum manometer and a VDG-1 vacuum meter, and spent gases had the following purities: Ne—99.996%, He—99.99%, Ar—99.992%, and Kr—99.999%. Hydrogen and deuterium (D_2 enrichment of 99%, nitrogen-impurity level of ~0.1%, and oxygen ~0.05%) were passed through silica gel and active copper for purification. The emission spectra were analysed by means of an SPM-2 monochromator with a quartz prism and an FEU-106 photomultiplier operating in photon-counting mode. The total activity of the α sources was 9.6 GBq, which corresponds to an average energy deposition of $W \sim 3 \cdot 10^{-5} \text{ W} \cdot \text{cm}^{-3}$ in 2 atm of helium and a “mean” ionisation rate of $S \sim 4 \cdot 10^{12} \text{ cm}^{-3} \text{ s}^{-1}$ with respect to the gas volume.

Studies of the luminescence spectra at higher pumping power and experiments with laser installations were conducted using a stationary nuclear reactor, WWR-K. WWR-K is a thermal neutron pool-type reactor. Its coolant, moderator, and reflector consist of desalted water. Uranium enriched to 36% in the isotope uranium-235 is used as reactor fuel. During the experiments, the maximum thermal-neutron flux density in the central channel of the reactor was $2 \cdot 10^{14} \text{ n/cm}^2 \cdot \text{s}$.

A diagnostic experimental installation (Figure 1) was arranged in the form of a stainless-steel tube that had been polished inside (1) with an outer diameter of 36 mm, a wall thickness of 2 mm, and a length of approximately 6 m, assembled from separate sections. The lower portion of the experimental installation, 700 mm in height, consisted of two concentric tubes with a gap of approximately 2 mm between them. The presence of such a double casing, the outer side of which was cooled by reactor water while the inner side was subjected to radiation heating, allowed the temperature of the ampoule that contained the gas mixture (2) to be adjusted by varying the pressure of the ^4He in the gap. The temperature at the bottom of the channel was controlled by a chromel-alumel thermocouple. This diagnostic experimental installation was loaded through a hole for a stopper in a rotating cast-iron reactor cover (3) and placed into the central channel of the core (4) of the nuclear reactor.

For the reactor research, gas mixtures were loaded into the core in vacuum-sealed glass ampoules, each of which had a window of radiation-resistant cerium glass [15]. The spectral range of measurement (350–830 nm) was determined by the transmission cut-off threshold of the window and the photomultiplier sensitivity. For measurements in the UV band, metal ampoules with sapphire windows were used. Tests have demonstrated that sapphire may be used as an exit window for lasers and for the investigation of the spectra of gas-mixture luminescence in the wavelength region from 0.2 to $7 \mu\text{m}$ and at neutron fluences of up to $10^{18} \div 10^{19} \text{ n/cm}^2$ [16]. For this purpose, it is preferable to use sapphire that does not contain chromium impurities, as when leucosapphire is used, the chromium R-line luminescence under intense γ radiation, even at a stalled reactor, impedes the measurement.

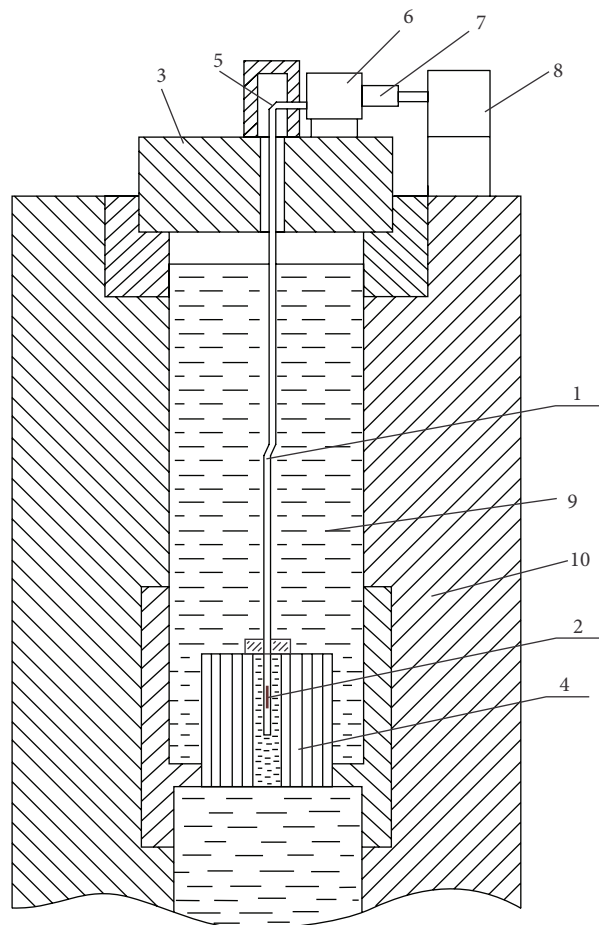


FIGURE 1: Installation for spectral studies on nuclear reactor. 1—experimental channel, 2—ampoule, 3—cast iron lid of the reactor, 4—the reactor core, 5—rotating mirror, 6—SPM-2 monochromator, 7—photomultiplier, 8—radiometer, 9—unsalted water, and 10—concrete protection.

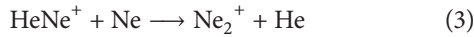
Three structures for laser installations inside the reactor core were developed and tested [17]. One structure was designed for testing xenon laser mixtures with pumping by uranium fission fragments; another was designed for testing lasers with inert gas mixtures excited by products of the $^3\text{He}(n,p)^3\text{H}$ reaction, and the third was designed for the creation of a laser at the mercury triplet lines. As discussed below, the pumping power under the experimental conditions at the WWR-K reactor proved to be insufficient to achieve lasing.

4. Active Media of Lasers at the p-s Transitions of Atoms

4.1. Mechanisms of Populating the p Levels of Inert Gas Atoms. The creation of a quasicontinuous laser pumped by an electron beam at the 3p-3s transitions of neon [18] inspired research on direct nuclear pumping. We conducted experiments to search for lasing at the neon transitions [8, 17] and researched a wide variety of ^3He -Ne-Kr(Ar)

mixtures at pressures of up to 7.5 atm. Our system made it possible to detect even spontaneous radiation of a mixture passing through the exit mirror. The lasing threshold was not achieved. Further theoretical research [19, 20] and experiments conducted by other organisations [21–23] indicated that the lasing threshold for the line at 585 nm exceeds 10^{14} n/cm²s.

The processes involved in the active media of lasers at the 3p-3s transitions of NeI are considered to be well studied [19, 24]: the population of the upper laser level occurs primarily because of the dissociative recombination of Ne_2^+ and HeNe^+ molecular ions. Under relatively weak pumping, HeNe^+ ions also form Ne_2^+ ions through the following substitution reaction:



Assuming that the dependence of the luminescence intensity of the line at 585 nm under radioisotope pumping is determined by the competition between processes involving the charge exchange of Ne_2^+ ions with the quenching additive and the recombination of electrons with Ne_2^+ , we can obtain the additive concentrations at which the intensity drops by a factor of 2:

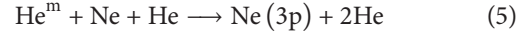
$$P = \frac{\sqrt{\beta \times S}}{k}, \quad (4)$$

where k is the coefficient of the Ne_2^+ charge exchange with the impurities and β is the coefficient of the Ne_2^+ recombination. Then, for $k \sim 10^{-10} \text{ cm}^3 \text{ s}^{-1}$ and $S \sim 4 \cdot 10^{12} \text{ cm}^{-3} \text{ s}^{-1}$, the presence of impurities at a level of $10^{-4}\%$ in an He-Ne mixture is sufficient to markedly decrease the intensity. In fact, the intensity at 585 nm in an He-Ne mixture decreases by a factor of 2 at an admixture pressure $0.4 \div 1.3 \text{ kPa}$ [8, 25].

Apparently, the population of the $3p'[1/2]_0$ level of NeI under excitation by heavy particles does not occur through the dissociative recombination of molecular ions. Adding up to 13.3 kPa of nitrogen with 2% O_2 impurities to an He(200 kPa)-Ne(6.7 kPa) mixture led to the same drop in intensity as for pure Ar and Kr [8, 25], indicating that the attachment of electrons to electronegative impurities had no effect on the population of the $3p'[1/2]_0$ level of neon. A similar result, also under radioisotope pumping, was obtained in [26]; the line intensity at 585 nm in a Ne(100 kPa)- O_2 (0.3 kPa) mixture was only 2 times lesser than the intensity of this line in neon at a pressure of 100 kPa, and the intensities of the lines at 703 and 725 nm were 4 times lesser. For comparison, in mercuric mixtures under nuclear pumping, the population of the HgI levels occurs through the dissociative recombination of the Hg_2^+ ions. Adding 10 Pa of oxygen to an ^3He -Hg mixture results in the attenuation of the triplet lines and the resonance line of mercury by a factor of ~ 500 [27]; this effect is attributed to electron attachment to O_2 .

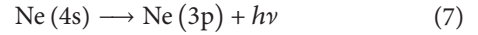
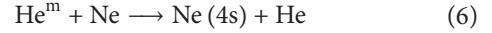
It was concluded that the population of the neon levels occurs under direct excitation by nuclear particles and secondary delta electrons. In He-Ne mixtures the population

also occurs through excitation transfer from metastable states of helium:



These conclusions were drawn on the basis of studying the spectral-temporal characteristics of pure neon and helium-neon under pumping by heavy charged particles [28].

From our point of view, the more probable channels for the population of the 3p levels in helium mixtures are cascade transitions from the 4s levels:



It is known that the $\text{Ne}(4s)$ levels are close to the $\text{He}(2^3\text{S}_1)$ level, and indeed, helium-neon laser operation at $1.15 \mu\text{m}$ is based on excitation transfer to neon atoms from $\text{He}(2^3\text{S}_1)$. The absence of the 4s-3p transition lines in high-pressure mixtures [28] is related to the fact that this transition is located in the IR region of the spectrum, beyond the photo-multiplier sensitivity limit. In one study [29], in which measurements were made at up to 1,100 nm, a line at 966.5 nm corresponding to the $4s[3/2]_2$ - $3p[1/2]_1$ transition was observed in neon and He-Ne mixtures under excitation by uranium fission fragments. Moreover, in the same study [29], more than 10 lines at the 3d-3p transitions were identified. The main conclusion of [25, 28] is that for neon-containing gas mixtures under pumping by heavy particles, the predominant mechanism for the population of the 3p levels of neon is not associated with the dissociative recombination of Ne_2^+ .

The excitation transfer to neon atoms from metastable atoms of helium and the direct excitation of neon by nuclear particles and secondary electrons are assumed [25] to be the most probable channels for $\text{Ne}(3p)$ population. In neon, the 3d, 4s, and 5s levels are excited by secondary electrons, and the population of $\text{Ne}(3p)$ occurs through cascade transitions from these levels. The 3d, 4s, and 5s levels, which are radiatively bound to the basic state, are effectively excited by electron impact. The lack of transition lines from the 5s levels observed in [10, 28] is attributable to the fact that the probability of 5s-3p transitions is much lower than the probability of 5s-4p transitions in the IR band of the spectrum. The 5s-4p, 4p-4s, and 4s-3p cascade transitions may also contribute to the population of the 3p levels of NeI. In helium-neon mixtures, the population of the 3p levels also occurs through the nonresonant transfer of excitation from the $\text{He}(2^3\text{S}_1)$ and $\text{He}(2^1\text{S}_0)$ metastable atoms to the 4s and 5s levels of neon and the subsequent cascade transitions.

Similar conclusions may be drawn with respect to mechanisms of level population in lasers with ionizing pumping at the nd -($n+1$)p transitions of inert gases ($n = 3, 4$, and 5 for argon, krypton, and xenon, resp.). According to [2, 30, 31], through the recombination of the molecular ions of argon, krypton, and xenon, the nd levels of atoms are populated, and the ($n+1$)p levels are populated through the subsequent cascade transitions of these nd levels. In [29], the luminescence spectra of the inert gases and their mixtures under pumping by uranium-235 fission fragments

were measured; the pumping power was $40 \text{ W} \cdot \text{cm}^{-3}$, which corresponded to a gas-ionisation rate of $10^{19} \text{ cm}^{-3} \text{ s}^{-1}$. When 1 kPa of krypton was added to 64 kPa of argon, the intensities of the lines at the 4p-4s transitions of argon atoms were lessened by a factor of 1.5; when 1 kPa of xenon was added, these intensities decreased by a factor of 2. At the 4p levels of the argon atom; the lifetime $\tau \approx 30 \text{ ns}$ corresponded to quenching by atoms of krypton and xenon, where the rate constant of quenching was approximately $10^{-10} \text{ cm}^3 \text{ s}^{-1}$. In the case of the recombination mechanism for the population of the 3d or 4p levels, the line intensities were decreased by 50–100 times as a result of the charge exchange of Ar_2^+ ions with the admixed impurities; the rate constants of the recharge of Ar_2^+ ions on atoms of Kr and Xe are reported in [32, 33].

The total line intensity of the 4p-4s transitions of argon atoms in the range of 696.5–842.5 nm decreased by only a factor of 1.5 upon the addition of 200 Pa of electronegative gas (NF_3) to 45 kPa of argon [34], confirming the conclusion that the recombination of molecular ions with electrons is not the basic mechanism of the population of the 4p and 3d levels of argon. The same conclusion may be drawn in relation to the 5p-5s transitions of krypton, as the lines intensity decreased only by a factor of 2 when 1 kPa of xenon was added to 32 kPa of krypton [29].

Therefore, the dissociative recombination of argon and krypton molecular ions with electrons is not the basic mechanism of the population of the $(n+1)p$ levels of atoms nor, correspondingly, the nd levels. The obtained results are consistent with the data [35, 36] concerning the predominant formation of Ar, Kr, and Ne atoms in the $(n+1)s$ or ground ($n p$) state upon the dissociative recombination of Ar_2^+ , Kr_2^+ , and Ne_2^+ ions.

4.2. Lasers at the 7s-6p Transitions of Mercury Atoms. The relatively high efficiency of lasers at the 3p-3s transitions of neon atoms under pumping by ionizing radiation with a low specific power of energy deposition ($\sim 10 \div 100 \text{ W/cm}^3$) motivated the search for novel collision lasers at allowed bound-bound electronic transitions. The triplet lines of the 7^3S_1 - $6^3\text{P}_{0,1,2}$ transition of the mercury atom ($\lambda = 546.1, 435.8, \text{ and } 404.7 \text{ nm}$, Figure 2) suggest themselves as prospective lines for lasers in the visible range because the upper level is sufficiently well excited by ionizing radiation [37, 38]. However, an attempt to depopulate the 6^3P_2 state by means of N_2 molecules following the scheme used in continuous lasers at $\lambda = 546.1 \text{ nm}$ under optical pumping by ionizing radiation was unsuccessful [37].

Another scheme for population inversion in lasers at the mercury triplet lines was proposed in [39]. It was shown that the population of the 7^3S_1 level of the mercury atom occurs through the dissociative recombination of ions but not through stepwise excitation by electrons [40]. When the partial pressure of deuterium in an He-Xe-Hg- D_2 mixture was increased to 13 kPa, the intensity of the resonance line of mercury weakened by more than a factor of 300, while the triplet line intensity fell by only a factor of 2.5. This finding indicates that the population of the HgI levels cannot be explained by stepwise excitation via resonance levels.

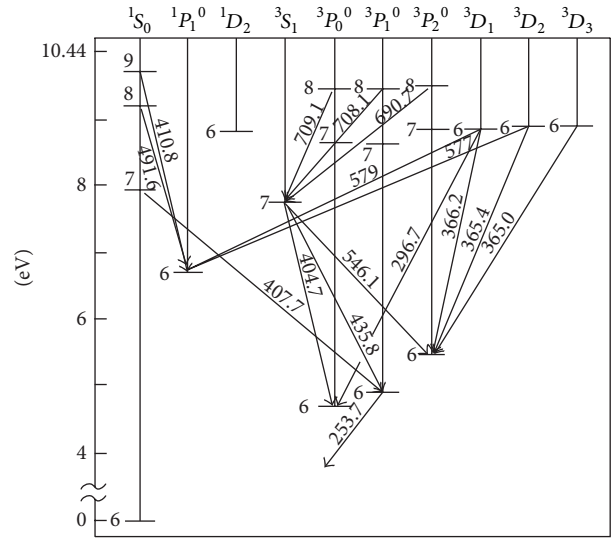
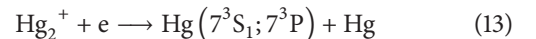
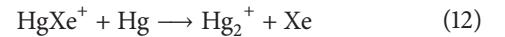
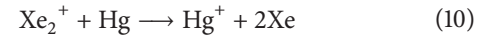
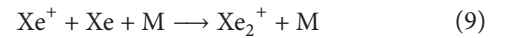
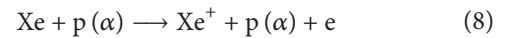


FIGURE 2: Scheme of the mercury atom levels. Wavelengths in nm are specified for the lines observed in spectrum of the ^3He -Hg mixture, excited by α -particles. Lines in the area of 313 nm are not shown.

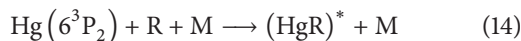
The intensity of the mercury triplet lines was nearly independent of the pressure of the mercury vapour, which was in the range of $0.1 \div 40 \text{ Pa}$ in the radioisotope installation and in the range of $0.1 \div 13 \text{ kPa}$ in the installation inside the reactor core, thus excluding any possibility of the direct excitation of the 7^3S_1 level from the ground state via electron impact. Based on these results, it is possible to conclude that electron impact is not the predominant mechanism for the population of the 7^3S_1 level of the mercury atom under excitation by hard ionizers. We believe it is most probable that dissociative electron-ion recombination is the primary channel for the population of the 7^3S_1 level in HgI under ionizing pumping. The most essential processes for this channel in an Xe-Hg plasma are as follows (where M represents the third type of particles):



The 7^3S_1 level is populated through the process described by (13) or through cascade transitions from the $7^3\text{P}_{0,1,2}$ levels. However, the wavelengths of these transitions lie beyond the sensitivity of the FEU-106 photomultiplier. The lack of cascade transitions from the 10^3P and 9^3P levels was reported in [37]. We have also determined that $8^3\text{P}_{0,1,2}$ - 7^3S_1 transitions are essentially absent [40].

Because the pumping is achieved through the ion channel, it is necessary to use xenon, whose charge exchange with hydrogen is slow, as a buffer gas. The use of krypton is less feasible because of the small value of the charge-exchange rate constant between Kr_2^+ ions and mercury atoms [41]. The high selectivity of the dissociative recombination of Hg_2^+ [38] is, to a large extent, conditioned by the low temperature of the electrons participating in recombination. Therefore, at a pumping power that is sufficiently high for laser operation, it is advantageous to use helium to cool the secondary electrons. It has been proposed that H_2 should be used for the lower-level depopulation at the $7^3\text{S}_1-6^3\text{P}_2$ transition and that H_2 and D_2 should be used at the $7^3\text{S}_1-6^3\text{P}_1$ transition. Therefore, the optimum operating mixture for a laser at the mercury triplet consists of four components: He, Xe, Hg, and H_2 [42]. At the WWR-K reactor, a mixture with a composition of ^3He (1 Amagat)-Xe (1 Amagat)- H_2 (0.04 Amagat)-Hg (1 Amagat, corresponding to gas density under normal conditions) was tested. The outlet temperature of the mercury was varied from 50 to 250°C (the partial pressure of the mercury vapour ranged from 1 Pa to 10 kPa), but the lasing threshold was not reached [8, 17].

Quasicontinuous lasing at the $7^3\text{S}_1-6^3\text{P}_2$ transition of the mercury atom using this type of scheme has been achieved at a pulse nuclear reactor [43]. A similar scheme has also been implemented for mixtures of mercury and inert gases under excitation by an electron beam [44]. In this study, an He-Ne-Ar mixture at a total pressure of 305 kPa was used as a buffer gas. An attempt to use H_2 for the population of the 6^3P_2 level was unsuccessful, and at a hydrogen pressure of 2.7 kPa, the laser action was lost. We believe that this occurred because molecular ions of helium that form in plasma are effectively recharged on Ar and Ne atoms (whose atomic ions are rapidly converted into molecular ions), Ar_2^+ and Ne_2^+ ions are recharged on H_2 , and the Ar_2^+ and Ne_2^+ charge-exchange rate constants with respect to Hg are small ($5 \cdot 10^{-11} \text{ cm}^3 \text{ s}^{-1}$ for Ne_2^+ and $<10^{-12} \text{ cm}^3 \text{ s}^{-1}$ for Ar_2^+ [41]). Because the mercury vapour pressure was only ~ 0.13 kPa, the beam energy was mostly consumed in the ionisation of H_2 , not the mercury atoms. The primary channel for mercury ionisation in such a mixture is the Penning process, which involves excited argon atoms. An interesting aspect of this study was the lack of lower-level quenching caused by the addition of dopant molecules. Depopulation of the lower laser level appeared to occur in the process of forming the excimer molecules (HgR) * :



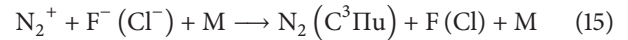
where R represents Ne or Ar.

In [43, 44], the recombination of the molecular ions of mercury with electrons is also considered to be the basic mechanism of the population of the 7^3S_1 level under ionizing pumping.

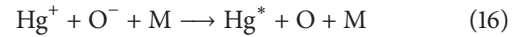
4.3. Population of Levels through Ion-Ion Recombination. In [45], it was proposed that the recombination of positive and

negative atomic ions can be used for laser pumping. Ion-ion recombination makes it possible to achieve high pumping selectivity, notably higher than that achievable through electron-ion recombination. Levels in the $0.3 \div 0.4$ eV range of energies are effectively populated, and at more widely spread energies, the cross-section diminishes rapidly. The use of ion-ion recombination under nuclear excitation is especially promising, as in this case, ions are primarily formed rather than excited states of atoms and ions. The possibility of creating a laser with direct nuclear pumping by exploiting ion-ion neutralisation was theoretically considered in [46]. Efforts were made to research the kinetics of populating the levels of atomic oxygen (nitrogen) through $\text{O}^- + \text{O}^+$ ($\text{O}^- + \text{N}^+$) neutralisation in $^3\text{He} + \text{N}_2\text{O} + \text{O}_2$ (N_2) mixtures. Negative ions of oxygen are formed through the attachment of electrons to molecules of nitrogen oxide. Although cross-section for ion-ion recombination decreases with increasing gas temperature, the cross-section of attachment grows much more rapidly with increasing temperature. Thus, an increase in the gas temperature should increase the effectiveness of the excitation of ion-ion recombination [46], which is essential in the radiation-heating conditions created in the presence of nuclear reactor radiation.

Experiments were conducted to investigate the population of the nitrogen molecule in the $\text{C}^3\Pi_u$ state in the following process:



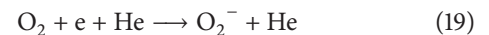
These experiments produced negative results [8, 27]. We also considered two processes involving negative ions of oxygen [27, 47]:



The emission spectra of $^3\text{He} + \text{Hg} + \text{CO}_2(\text{O}_2)$ gas mixtures under excitation by α particles of ^{210}Po were studied. In the experimental conditions, the predominant channel for the formation of negative ions in mixtures containing CO_2 was dissociative attachment:



In mixtures containing O_2 , the predominant channel was attachment through triple collisions:



The line intensities observed in mixtures of ^3He (200 kPa) and Hg (0.2 kPa) with the addition of O_2 and CO_2 are presented in Table 1. The strengthening of the lines in the range of 366 ± 1 nm that was observed with increasing CO_2 pressure can be explained by the increase in the CO_2^+ ion transition intensity at $\lambda = 367$ nm (the intensity of the band at 351 nm is provided for comparison). The significant reduction of the line intensity of the transitions from the 6D levels and the moderate increase in the line intensity of the mercury triplets

TABLE 1: Relative line intensities in mixtures containing mercury.

Mixture	Wavelength (nm) and transition					
	253 $6^1S_0-6^3P_1$	297 $6^3P_0-6^3D_1$	313 6^3P_1-6D	365 ÷ 367 $6^3P_2-6D/(CO_2^+)$	436 $6^3P_1-7^3S_1$	351 (CO_2^+)
$^3He + Hg$	14000	540	930	1000 (365 nm) 2200 (366 nm)	25500	2000
$^3He + Hg + CO_2$ (13 Pa)	8000	150	400	7400	32000	5800
$^3He + Hg + CO_2$ (130 Pa)	1400	20	50	650	9700	600
$^3He + Hg + O_2$ (13 Pa)	~30			907	~60	926
$^3He + Hg + O_2$ (130 Pa)	~0			~0	~0	0

observed with the increase in the partial pressure of CO_2 lead to the following hypotheses.

The rapid attenuation of the mercury triplet lines in the oxygen-containing mixtures can be explained by the attachment of electrons to molecules of O_2 (and, partially, by the level quenching caused by the oxygen molecules). This finding once again confirms the population mechanism of the 7^3S_1 level of the mercury atom to be dissociative electron-ion recombination.

4.4. Emission of 3He -Xe-Cd Mixtures. The energy-level scheme of the cadmium atom is similar to that of mercury (Figure 3). Therefore, the study of the feasibility of quasicontinuous lasing at the 6s-5p transitions of Cd is of some interest [15]. The quantum-efficiency coefficient of such a system (the ratio of the photon energy to the energy required to form an electron-ion pair with Xe or Kr) is greater than 10%, which is notably higher than that of the cadmium-ion transitions in He-Cd mixtures. The laser effect at the cadmium triplet lines was achieved through transverse discharge in an He-Cd- H_2 mixture [48]. Hydrogen quenches the 5^3P_1 level of the Cd atom. Laser action was achieved in the discharge afterglow, indicating that a recombination mechanism drove the population of the upper laser level.

The excitation spectrum of an 3He -Cd mixture in a nuclear reactor core [15] is generally consistent with that described in [37], although the relative intensities of certain lines differ. A continuous spectrum is formed by radiation from Cd_2^+ molecules. In addition to lines associated with the cadmium triplet and the 643.8 nm ($5^1D_2-5^1P_1$) line of atomic cadmium, the 361.0 nm ($5^3D_3-5^3P_2$) line was also observed. Its intensity reached a maximum (at 350°C) of approximately 5.5 units. For comparison, the maximum intensity of the ion line of 441.6 nm, the brightest line under our experimental conditions, was 110 units at 360°C.

In an 3He -Xe-Cd mixture, the intensity of the line at 361.0 nm is below the sensitivity threshold of the experimental setup (~0.1 units); thus, as expected, the Cd II lines were not observed. The population of the cadmium levels 6^3S_1 and 5^1D_2 may occur both directly, through the recombination of Cd_2^+ ions with electrons and through cascade processes from higher levels. The wavelengths of such transitions lie beyond the photomultiplier sensitivity by approximately. Lasing at the $6^3P_1-6^3S_1$, $4^3F_2-5^3D_3$ transitions under the pumping of

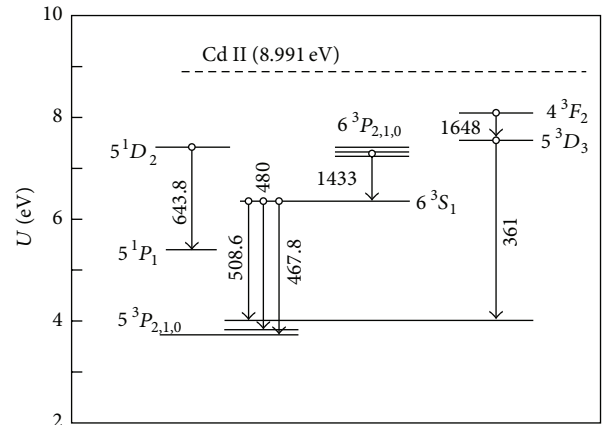


FIGURE 3: Scheme of some levels of cadmium atom.

an He-Cd mixture by uranium fission fragments was reported in [49], and similarly, laser action under pumping by an electron beam at $\lambda = 361$ nm was reported in [50]. The absence of the 361.0 nm line in the radiation spectrum indicates that in (He)-Xe-Cd mixtures, either the population of the 4^3F_2 and 5^3D_3 levels is not essential or these levels are strongly quenched by xenon. The temperature dependence of the intensities of the lines at 508.6 and 643.8 nm indicates that the recharging of Xe_2^+ on Cd is slow. The dependence of the intensity at $\lambda = 508.6$ nm upon the density of cadmium atoms (N) is illustrated in Figure 4. The dependence of the intensity on N , similar to the case for Hg, is described by the following expression [15, 47]:

$$I = \frac{kN}{kN + \sqrt{\alpha S}} I_{\infty}, \quad (20)$$

where I_{∞} is the intensity at a high density of cadmium atoms, k is the rate constant for the recombination of Cd_2^+ ions, and α is the coefficient of electron-ion recombination, which is accepted to be the same as for basic ions ($\approx 10^{-6} \text{ cm}^3 \text{ s}^{-1}$). The rate of gas ionisation ($S \approx 10^{16} \text{ cm}^{-3} \text{ s}^{-1}$) was evaluated based on known cross-sections of nuclear reactions and the ranges of protons and tritons in gas. The correlation between (20) and the experimentally observed dependence (see Figure 3) yields $I_{\infty} \approx 200$ units and $k \sim 10^{-13} \text{ cm}^3 \text{ s}^{-1}$.

Therefore, the rate constant for the recharging of Xe_2^+ on cadmium atoms is insignificant compared to the constant for

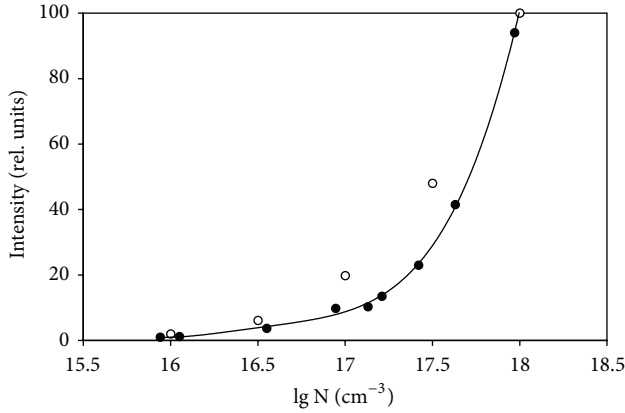


FIGURE 4: Dependence of intensity of the 508.6 nm line on the vapor density of cadmium in the $^3\text{He-Xe-Cd}$ mixtures. Open circles—calculation by formula (20) for $I_\infty = 200$ units, $k = 10^{-13} \text{ cm}^3 \text{ s}^{-1}$.

recharging on mercury atoms. A cadmium vapour density that is sufficiently high for charge exchange with Xe_2^+ ions ($\sim 3 \cdot 10^{18} \text{ cm}^{-3}$) is created at temperature of approximately 700°C . At such a cadmium density, it is necessary to take into consideration the quenching of the 6^3S_1 state by atoms of cadmium itself, although in the density range we investigated, no significant quenching was detected (see Figure 3). It is quite possible that in krypton, recharging on Cd will occur more rapidly. Furthermore, in krypton, cadmium atoms may ionize through the Penning process.

5. Emission of Nuclear-Induced Plasma at Molecular Transitions

Wide molecular-transition bands lead to high values of the threshold pumping power, making it difficult to create a molecular laser based on nuclear pumping at the stationary reactor. Spectral research was conducted to determine the kinetics of the plasma-induction process in gas mixtures that were considered to be candidates for the active media in molecular lasers excited by pumping from pulse nuclear reactors or electron beams. Radioluminescence at the molecular transitions in gas mixtures is also of interest with respect to nuclear sources of incoherent radiation and radiation photochemical synthesis.

The most important results at INP were obtained by studying the spectrum of the first negative system of CO, the radiation of heteronuclear ionic molecules of inert gases, and the luminescence of halogenides of inert gases. Following a publication concerning the creation of an efficient (efficiency coefficient of $\sim 2\%$) quasicontinuous laser at high pressure based on the first negative system of nitrogen [51], efforts commenced to research the corresponding system of CO [52, 53]. A pulse discharge laser based on the 1^- system of CO was first implemented in 1975 [54], but no further investigations of the active medium of a CO^+ laser were conducted. The molecular bands of Ar-Xe and Kr-Xe mixtures under excitation by electron beams were first detected half a century ago [55, 56], but at that time, they were not correctly interpreted.

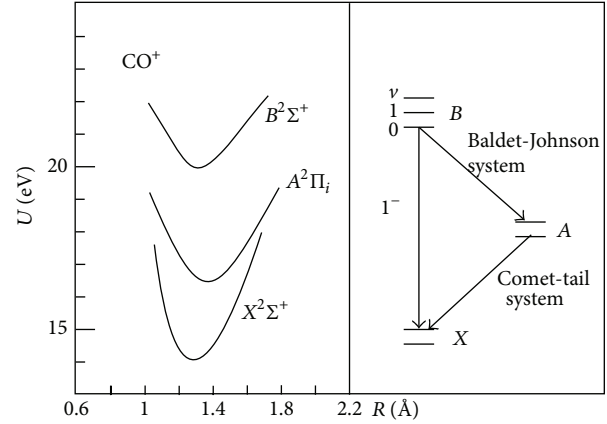


FIGURE 5: Scheme of electronic terms and transitions of the CO^+ molecule.

Research has also been conducted under pumping by α particles [57]. In our work [58], the high efficiency of $(\text{ArXe})^+$ and $(\text{KrXe})^+$ luminescence was observed for the first time. In a later study, we conducted detailed research concerning Ar-Xe and Kr-Xe emission under nuclear pumping [14, 59]. The luminescence of inert-gas halogenides was researched [16, 60] in connection with attempts to create an excimer laser based on pumping by a pulse nuclear reactor [61, 62].

5.1. Kinetics of Excitation of the First Negative System of CO.

The creation of a quasi-continuous laser in the UV range based on the first negative system of CO (Figure 5) is of interest because the quantum-efficiency coefficient for the $0-1$ ($\lambda = 230 \text{ nm}$) transition is 12.7%, and the population efficiency of the upper laser level of $B^2\Sigma_u^+$ is significant [52, 53]. Hydrogen and deuterium molecules and krypton atoms have high rate constants for the depopulation of the lower level, $X^2\Sigma_g^+$ [63]. It should be noted that ions of COH^+ (similar to COD^+) form through transitions of heavy particles:



These COH^+ ions do not absorb radiation in the first negative system of CO [64]. Consequently, $\sim 400 \text{ Pa}$ of hydrogen or krypton is quite sufficient for the depopulation rate of the lower laser level to exceed the rate of spontaneous decay of the upper level ($\nu = 1.92 \cdot 10^7 \text{ s}^{-1}$ [64]) by an order of magnitude. Thus, the possibility of creating a quasicontinuous laser at the B-X transition of CO^+ is determined by the correlation between the depopulation rates of the upper and lower laser levels associated with H_2 and D_2 molecules and Kr atoms. To determine the efficiency of population and the rate constants of depopulation attributable to such quenching dopants, it is first necessary to determine the self-quenching rate of $\text{CO}^+(B)$ and the quenching attributable to buffer gases.

Quenching of the B-State of CO^+ by Helium, Neon, and CO.

The rate constants of $\text{CO}^+(B)$ quenching were determined based on the dependence of the luminescence intensity of the

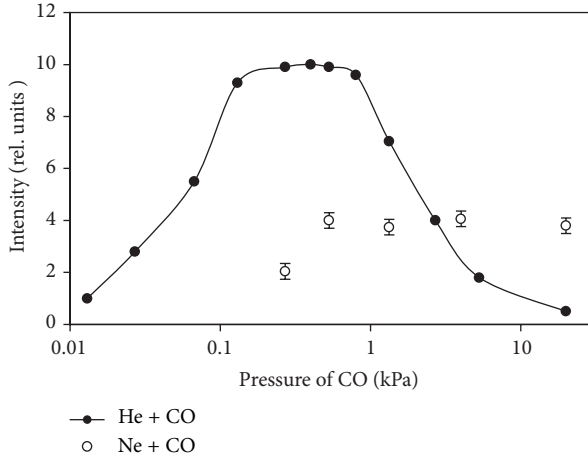
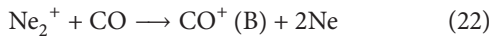


FIGURE 6: Intensity on 230 nm versus pressure of CO in He (400 kPa) + CO and Ne (122 kPa) + CO.

first negative system of CO on the partial pressures of gases in the mixture. The maximum radiation intensity at 230 nm in an He(400 kPa)-CO mixture was achieved at a CO pressure of $0.1 \div 0.8$ kPa (Figure 6). The dependence of the luminescence intensity on the CO pressure indicates significant quenching of $\text{CO}^+(\text{B})$ in two- and/or three-particle collisions with CO and He. The intensity of the bands of the 1^- system of CO in an Ne(120 kPa) + CO(0.53 kPa) mixture is approximately 2.5 times lower than the intensity of the bands in an He (400 kPa) + CO(0.53 kPa) mixture (see Figure 6); the pressures of the mixtures were selected to ensure equal α -particle ranges and, correspondingly, equal mixture pumping powers. In addition, in the Ne-CO mixture, there were no B-X transitions of CO^+ from the $v' > 0$ levels. The obtained values of the rate constants of $\text{CO}^+(\text{B})$ quenching are presented in Table 2.

It can be seen from the data that the lower intensity of the luminescence at the B-X transition of CO^+ in the Ne-CO mixture compared with that in He-CO is attributable to the drastic quenching of the B state by neon, not by the weakness of the following process:



The absence of $v' > 0$ lines in the emission spectrum of the Ne-CO mixture is related to the fact that the rate constant of the quenching of the $\text{B}^2\Sigma_{u,v'}^+$ state by neon for $v' = 1, 2$ is approximately 5 times higher than that for the main vibration state.

Efficiency of the Population of $\text{CO}^+(\text{B})$. The population efficiency of the $\text{B}^2\Sigma_{u,v'=0}^+$ level was determined based on the correlation between the intensities for the first negative system of N_2 and the Baldet-Johnson system. The bands under investigation lie in a suitable range of wavelengths (391.4 and 427.8 nm for N_2^+ and 395 and 420 nm for CO^+), where the response of the experimental apparatus was maximal. The band-intensity ratio was measured for He (400 kPa) + N_2 (53 Pa) and He (400 kPa) + CO mixtures. The P-band branches of the Baldet-Johnson system were forbidden and

overlapped with the relevant Q-band edges. The total intensity of the 1^- system of CO transitions from the $v' = 0$ level was determined by taking into account the branching coefficient of the transition for $\text{B}^2\Sigma_u^+$, $\delta = 8\%$ [65]. The ratio of the number of quanta radiated by the B-A transitions of CO^+ ions to the number of quanta radiated by the first negative system of N_2 at the same helium pressure was determined using the following expression:

$$\frac{I_{\text{N}_2}}{I_{\text{CO}}} = \frac{\chi}{\eta} \cdot \frac{v + k_1[\text{CO}] + k_2[\text{He}] + k_3[\text{CO}][\text{He}]}{v_{\text{N}_2} + k_{1\text{N}_2}[\text{N}_2] + k_{2\text{N}_2}[\text{He}] + k_{3\text{N}_2}[\text{N}_2][\text{He}]} \cdot \frac{v_{\text{N}_2}}{v}, \quad (23)$$

where $\chi = 0.75$ is the population efficiency $\text{N}_2^+(\text{B}_{v'=0})$ for two- and three-particle processes of charge exchange on nitrogen [66], $v_{\text{N}_2} = 1.58 \cdot 10^7 \text{ s}^{-1}$ [64] is the rate of spontaneous decay of $\text{N}_2^+(\text{B})$, $k_{1\text{N}_2}$ and $k_{2\text{N}_2}$ are the rate constants for $\text{N}_2^+(\text{B})$ quenching in two-particle collisions with N_2 and He and $k_{3\text{N}_2}$ is the rate constant for the three-particle process with N_2 and He [67]. By comparing the measured value of $I_{\text{B-A}}/I_{\text{N}_2}$ to that calculated using formula (23), we obtained $\eta \sim 0.2$. The relative efficiencies of population of certain $\text{CO}^+(\text{B})$ vibration levels were determined based on the intensities of the 0-2, 1-3, and 2-4 transitions of the 1^- system. These transitions lie in a narrow range of the spectrum (242–247 nm) where the spectral response of the experimental apparatus could be considered to be constant. For the He (400 kPa) + CO (5.3 kPa) mixture, the following population efficiencies were obtained for the vibration levels: $\eta_{v'} = 63\%$ for the $v' = 0$ level, $\eta_{v'} = 27\%$ for the $v' = 1$ level, and $\eta_{v'} = 10\%$ for the $v' = 2$ level.

Recharging of He_2^+ on Hydrogen, Deuterium, Krypton, and Carbon Monoxide. To evaluate the rates of $\text{CO}^+(\text{B})$ quenching caused by H_2 , D_2 , and Kr, it is necessary to know the constants related to “parasitic” processes. It is known that the recharging of He^+ on H_2 and D_2 is nearly nonexistent and that the rate constant for the corresponding process with krypton, by analogy with Ar and Xe, should also be small [63]. Thus, the recharging of He_2^+ on H_2 , D_2 , and Kr should be the predominant “parasitic” processes. Because the luminescence of He- N_2 mixtures has been studied more thoroughly than that of He-CO, the rate constants for the recharging of He_2^+ were determined based on the dependence of the backward intensity of the $\text{N}_2^+(\text{B-X})$ luminescence in an He- N_2 mixture on dopant pressure [67]. The results are summarised in Table 3.

Constants k_7 , k_{10} , and k_{13} are in good agreement with those obtained in [68, 69]. At the same time, we believe that the rate-constant values for the three-particle process for the recharging of He_2^+ on Kr and CO presented in [68, 69] are too high for a helium-pressure range of $1 \div 6$ atm.

$\text{CO}^+(\text{B})$ Quenching by Hydrogen, Deuterium, and Krypton. In Figure 7, the dependence of the intensity of the first negative

TABLE 2: Rate constants of $\text{CO}^+(\text{B})$ quenching [53].

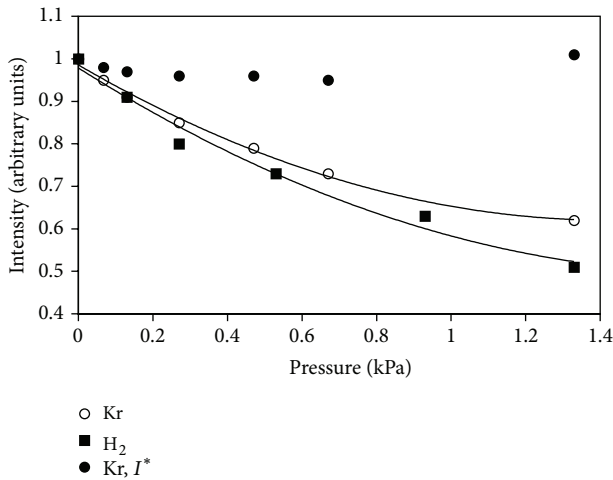
Process	Notation, units ($\text{cm}^3 \text{s}^{-1}$, $\text{cm}^6 \text{s}^{-1}$)	Rate coefficient
$\text{CO}^+(\text{B}_{v=0}) + \text{CO} \rightarrow \text{products}$	$k_1, 10^{-11}$	~ 2
$\text{CO}^+(\text{B}_{v=0}) + \text{He} \rightarrow \text{products}$	$k_2, 10^{-13}$	5 ± 2
$\text{CO}^+(\text{B}_{v=0}) + \text{CO} + \text{He} \rightarrow \text{products}$	$k_3, 10^{-30}$	2 ± 1
$\text{CO}^+(\text{B}_{v=0}) + \text{Ne} \rightarrow \text{products}$	$k_4, 10^{-11}$	1.5 ± 0.5
$\text{CO}^+(\text{B}_{v=1}) + \text{Ne} \rightarrow \text{products}$	$k_{41}, 10^{-11}$	~ 8
$\text{CO}^+(\text{B}_{v=2}) + \text{Ne} \rightarrow \text{products}$	$k_{42}, 10^{-11}$	~ 7

TABLE 3: Rate constants for processes involving He_2^+ .

Process	Notation, units ($\text{cm}^3 \text{s}^{-1}$, $\text{cm}^6 \text{s}^{-1}$)	Rate coefficient	References
$\text{He}_2^+ + \text{N}_2 \rightarrow \text{products}$	$k_5, 10^{-10}$	11 ± 3	[68]
$\text{He}_2^+ + \text{N}_2 + \text{He} \rightarrow \text{products}$	$k_6, 10^{-30}$	16 ± 3	[68, 70]
$\text{He}_2^+ + \text{Kr} \rightarrow \text{products}$	$k_7, 10^{-11}$	8 ± 3 ≤ 8	* [69]
$\text{He}_2^+ + \text{Kr} + \text{He} \rightarrow \text{products}$	$k_8, 10^{-30}$	3 ± 1 17 ± 3	* [69]
$\text{He}_2^+ + \text{H}_2 \rightarrow \text{products}$	$k_9, 10^{-10}$	10 ± 3 4.1 ± 1.2 $5.3 (200 \text{ K})$ 24 ± 4	* [69] [63] [70]
$\text{He}_2^+ + \text{H}_2 + \text{He} \rightarrow \text{products}$	$k_{10}, 10^{-30}$	15 ± 5 9 ± 5 1	* [68] [71]
$\text{He}_2^+ + \text{D}_2 \rightarrow \text{products}$	$k_{11}, 10^{-10}$	8 ± 3	*
$\text{He}_2^+ + \text{D}_2 + \text{He} \rightarrow \text{products}$	$k_{12}, 10^{-30}$	< 2	*
$\text{He}_2^+ + \text{CO} \rightarrow \text{products}$	$k_{13}, 10^{-10}$	13 ± 4 11 14	* [68] [63]
$\text{He}_2^+ + \text{CO} + \text{He} \rightarrow \text{products}$	$k_{14}, 10^{-30}$	2 ± 1 36 ± 8	* [68]

*Data from [67].

Here and in Table 4, the constant values marked in bold were used as references.

FIGURE 7: Dependence of the intensity at 230 nm on the pressure of hydrogen or krypton. I^* —modified intensity, estimated by the formula (24).

system of CO on the pressure of H_2 or Kr is depicted. For Kr, the modified intensity is also given:

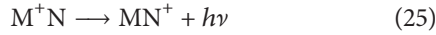
$$I^* = I \frac{k_7 [\text{Kr}] + k_8 [\text{Kr}] [\text{He}] + k_{13} [\text{CO}] + k_{14} [\text{CO}] [\text{He}]}{k_{13} [\text{CO}] + k_{14} [\text{CO}] [\text{He}]} \quad (24)$$

This quantity accounts for the competition between the He_2^+ recharging processes on CO and Kr. It can be seen that the decrease in intensity that accompanies the increase in dopant pressure to 2.7 kPa can be explained (within $\sim 15\%$ error) by the influence of parasitic processes. Then, when the rate constants for $\text{CO}^+(\text{B})$ quenching in collisions with CO and He (see Table 2) are known, it is possible to evaluate the upper limit on the rate constant for $\text{CO}^+(\text{B})$ quenching by H_2 and D_2 molecules or atoms of krypton: $k_q < 10^{-10} \text{ cm}^3 \text{s}^{-1}$.

Thus, the rate of depopulation of the upper laser level caused by hydrogen and krypton is, at least, 20 times lower than that of the lower laser level. The population efficiency of the $\text{B}_{v=0}$ state of CO^+ was found to be low ($\eta \sim 0.2$)

in comparison with the population efficiency of $N_2^+(B)$ in the helium-nitrogen mixture. However, it is true that the quenching of the B state of CO^+ by helium is lower than that for $N_2^+(B)$ by a factor of 2. Most importantly, the population depends on the A- and X-states of CO^+ . Thus, for the creation of a laser, it is preferable to consider the 0-1 and 0-2 transitions ($\lambda = 230$ nm and $\lambda = 242$ nm) rather than the 0-0 transitions of the first negative system of CO. We should note that in [54], amplification was observed exactly at the 0-2 transition. Because of the relatively low selectivity of the $CO^+(B)$ population, we expect that the optimum dopant pressure for quenching will most likely be considerably higher than 400 Pa.

5.2. Emission of Heteronuclear Ionic Molecules of Inert Gases. The molecular bands that were observed in the radiation spectra of binary mixtures of inert gases [55, 56] were identified [72] as transitions between states of heteronuclear ionic molecules:

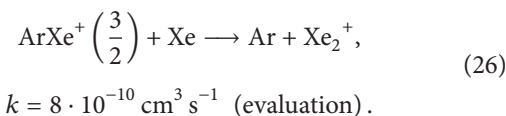


where the molecular states M^+N asymptotically correspond to the states $M^+ + N$ and MN^+ corresponds to the states $M + N^+$; here, M and N are atoms of inert gases, and N is the heavier atom. If up to 5 such bands are observed in a low-pressure plasma in the electric discharge of binary mixtures of inert gases [72], then in a mixture at medium or high pressure under excitation by ionizing radiation, there are no transitions from levels corresponding to the $^2P_{3/2}$ states of the atomic ions [57, 58]. Because of the high selectivity of excitation, the emission of heteronuclear ionic molecules of inert gases is of interest for the direct transformation of nuclear energy into coherent or incoherent optical radiation [58, 73].

Argon-Xenon. The major kinetic processes of the formation and decay of $Ar^+(1/2)Xe$ ions in Ar-Xe mixtures are summarized in Table 4.

The absence of radiation at the transitions from the $Ar^+(3/2)Xe$ level is explained [57] by the large difference between the rate coefficients of the process (2t) competing with $Ar^+(1/2)Xe$ formation and the corresponding process (9t) for $Ar^+(3/2)$ ions. The rate coefficient for the conversion of $Ar^+(3/2)$ ions to molecular ions is approximately 50 times higher than that for $Ar^+(1/2)$ ions (see Table 4). It is possible that the rate constants of other processes that contribute to the formation and decay of $Ar^+(3/2)Xe$ are also significantly different.

The high selectivity of excitation of the band at 329 nm [58], in combination with the weak quenching of the upper level, suggests the possibility of creating a laser at this transition. The lower level is effectively depopulated through the following process:



Let us evaluate the lasing threshold, without taking into account the nonresonance losses. The unsaturated coefficient of amplification can be determined from the following relations:

$$\alpha = \sigma n \approx \sigma \frac{W}{E_u} \tau_u = \frac{\lambda^4}{4\pi^2 c} \frac{A \tau_u}{\Delta \lambda} \frac{W}{E_u}, \quad (27)$$

where σ is the cross-section of the stimulated transition, W is the pumping power, $E_u = 78$ eV is the energy consumed to form one ion of $Ar^+(1/2)$, τ_u is the lifetime of upper level with taking into account the quenching by xenon atoms, $\Delta \lambda = 2.5$ nm is the half-width of the band at 329 nm, and A is the probability of the transition. Then, the threshold pumping power for the Ar (100 kPa) + Xe (6.7 kPa) mixture is

$$W_{th} = \frac{4\pi^2 c \Delta \lambda}{\lambda^4} \frac{\alpha_0 E_u}{A \tau_u} \approx 3 \text{ kW} \cdot \text{cm}^{-3}, \quad (28)$$

where α_0 is the threshold coefficient of amplification; the value assumed here is $\alpha_0 = 10^{-3} \text{ cm}^{-1}$. Despite the relatively low lasing threshold, lasing at this transition was not achieved for an Ar-Xe mixture under pumping by an electron beam [58, 73]. It appears that the lack of any laser effect can be explained by the strong absorption by Xe_2^+ ions and the decreased excitation selectivity of $Ar^+(1/2)Xe$ under powerful pumping. We believe that the upper level quenching caused by the argon atoms [73] is insignificant (see Table 4).

Krypton-Xenon. In the luminescence spectrum of a Kr-Xe mixture luminescence, a known band at approximately 445–510 nm (490 nm band) was observed [59] that corresponds to the transition between $(KrXe)^+$ states with dissociation limits of $Kr^+(^2P_{1/2}) + Xe(^1S_0)$ {hereafter $Kr^+(1/2)Xe$ } and $Kr(^1S_0) + Xe^+(^2P_{3/2})$ {hereafter $KrXe^+(3/2)$ }. At atmospheric pressure, there is no band at $\lambda \sim 660$ nm that corresponds to the transition from the $Kr^+(3/2)Xe$ state. The remaining expected bands lie in the infrared region (approximately 1.0 to 2.2 μm). The wavelengths of these transitions were estimated [72] from the energy levels of Kr^+ and Xe^+ . Two emission systems were observed, in the 600–670 and 670–685 nm regions, when Xe was added to a Kr flowing afterglow at a pressure of 30 Pa [74].

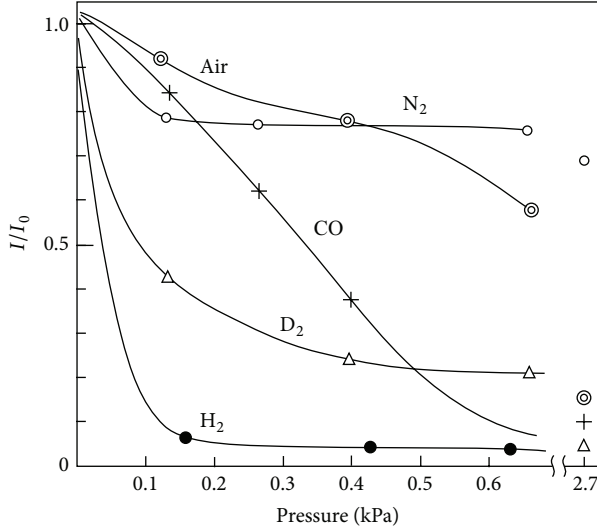
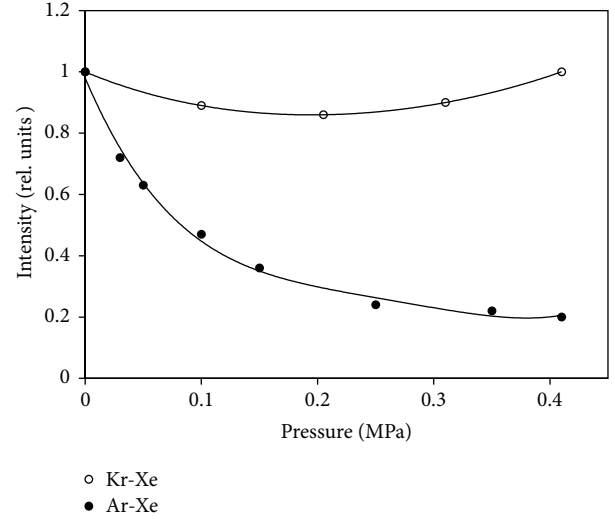
Intense luminescence of the band at 490 nm was observed even after adding several hundred Pascal of krypton to xenon, although the optimum ratio of a Kr-Xe mixture with respect to the emission intensity is Kr : Xe = 1 : 1. Measurements with α sources have demonstrated that the luminescence intensity of a Kr : Xe = 1 : 1 mixture remains constant at temperatures ranging from indoor room temperature up to $\approx -100^\circ\text{C}$. At lower temperatures, a rapid decrease in intensity was observed, which was apparently related to the freezing of the xenon. Measurements at temperatures than 40°C were performed using the in-core experimental installation. The initial partial pressures of the gases in the ampoule were as follows: ^3He —13 kPa, Kr—33 kPa, and Xe—33 kPa. The luminescence intensity decreased by a factor of 2 at an ampoule temperature of $t_a \sim 350^\circ\text{C}$, and the radiation at $\lambda = 490$ nm disappeared at $t_a \sim 600^\circ\text{C}$.

Figure 8 illustrates the effects of the molecular dopants on the radiation intensity of the band at 490 nm under excitation

TABLE 4: Rate constants for processes in Ar-Xe-(He) mixtures.

N	Process	Notation, units ($\text{cm}^3 \text{s}^{-1}$, $\text{cm}^6 \text{s}^{-1}$)	Rate coefficient	References
1t	$\text{Ar}^+(1/2) + \text{Xe} + \text{Ar} \rightarrow \text{products}$	$k_{15}, 10^{-31}$	5.2	[57]
	$\text{Ar}^+(1/2) + \text{Xe} + \text{Ar} \rightarrow \text{Ar}^+(1/2)\text{Xe} + \text{Ar}$	ρk_{15}	$0.16 \leq \rho \leq 0.7$ $\rho \sim 1$	[73] *
2t	$\text{Ar}^+(1/2) + 2\text{Ar} \rightarrow \text{products}$	$k_{16}, 10^{-33}$	0.72 7 ± 2	[57] *
3t	$\text{Ar}^+(1/2) + 2\text{Xe} \rightarrow \text{products}$	$k_{17}, 10^{-32}$	3.4	[57]
4t	$\text{Ar}^+(1/2)\text{Xe} \rightarrow \text{ArXe}^+(3/2) + h\nu$	τ, ns	58	[73]
5t	$\text{Ar}^+(1/2)\text{Xe} + \text{Ar} \rightarrow \text{products}$	$k_{18}, 10^{-11}$	3.2 <0.05	[73] *
6t	$\text{Ar}^+(1/2)\text{Xe} + \text{Xe} \rightarrow \text{products}$	$k_{19}, 10^{-12}$	<10 ~ 1	[73] *
7t	$\text{Ar}^+ + \text{Xe} \rightarrow \text{Xe}^+ + \text{Ar}$	$k_{20}, 10^{-13}$	9.8	[73]
8t	$\text{Ar}^+(1/2)\text{Xe} + \text{He} \rightarrow \text{products}$	$k_{21}, 10^{-13}$	6 ± 2	*
9t	$\text{Ar}^+(3/2) + 2\text{Ar} \rightarrow \text{products}$	$k_{22}, 10^{-31}$	3	[57, 63]

*Data from [14].

FIGURE 8: Dependence of the intensity of radiation at $\lambda = 490 \text{ nm}$ on the pressure additives to the mixture Kr(55 kPa)-Xe(55 kPa).FIGURE 9: Dependence of the intensity of radiation on the helium pressure in a mixture of Kr(55 kPa)-Xe(55 kPa)-He at $\lambda = 490 \text{ nm}$ and in a mixture of Ar(135 kPa)-Xe(15 kPa)-He at $\lambda = 329 \text{ nm}$.

by α particles. During the measurements collected using the in-core installation, hydrogen and tritium were produced in the ampoule as a result of the nuclear reaction ${}^3\text{He}(n,p){}^3\text{H}$. By the time the temperature-dependence measurements were completed, the thermal-neutron fluence had reached $\sim 9 \cdot 10^{16} \text{ n}\cdot\text{cm}^{-2}$. Thus, based on the known nuclear-reaction cross-section (5400 barns), the density of the produced hydrogen and tritium can be estimated to have been $\sim 1.6 \cdot 10^{15} \text{ cm}^{-3}$, which corresponds to 7 Pa at room temperature. This number of isotopes could not have significantly affected the intensity of the 490 nm band (see Figure 8). Through α decay, helium was produced in the mixture. Therefore, the influence of helium-4 on the emission intensities of the Kr-Xe mixture and, for comparison, an Ar-Xe mixture at $\lambda = 329 \text{ nm}$ (Figure 9) were measured. The measurements

indicated that upon adding air, CO, N_2 , H_2 , or D_2 at pressures of up to 2.7 kPa and He at a pressure of up to 400 kPa into the Kr-Xe mixture, no luminescence appeared at $\lambda \sim 660 \text{ nm}$. The coefficient of the transformation of nuclear energy into photoenergy (η) was determined by comparing the intensity of the band of interest with the intensity of the $\text{C}^3\Pi_u - \text{B}^3\Pi_g$ band in the Ar- N_2 mixture. For the Kr: Xe = 1:1 mixture at a pressure of 110 kPa, the value $\eta = 11 \pm 4\%$ was obtained. The mechanism of the processes, similar to the case of Ar-Xe mixtures, cannot explain the rapid increase in intensity observed upon adding krypton to xenon [59]. The intensity observed for the mixture with 0.7% Kr constitutes 10% of the intensity observed for the Kr: Xe = 1:1 mixture, although in the latter case, almost all the energy was used to ionize and excite the Xe atoms. The high efficiency of radiation at

$\lambda = 490 \text{ nm}$ and the continued presence of luminescence through a mixture temperature of $\sim 600^\circ\text{C}$ serve as strong evidence that the bonding-energy value for $\text{Kr}^+(1/2)\text{Xe}$ ($\sim 0.009 \text{ eV}$) given in [75] is lower than the true value. The kinetics of the processes in a Kr-Xe mixture excited by ionizing radiation require further research.

5.3. Luminescence of Inert-Gas Halogenides. Currently, excimer lasers based on inert-gas halogenides are the most powerful lasers that radiate in the UV region of the spectrum. The optimum operation mode of excimer lasers corresponds to pumping powers of several megawatts per cm^3 and pressures of several atmospheres. Such pumping powers are achieved by means of electron beams or electrical discharge. The creation of an excimer laser based on nuclear pumping is of interest when the energy of the nuclear-reaction products is directly transferred to the active medium of the laser but the pumping power does not exceed 10 kW/cm^3 [61, 62].

We have studied the emission spectra of inert-gas mixtures with NF_3 and CCl_4 under excitation by α particles from ^{210}Po [60]. The emission spectra of the inert-gas mixtures with halogenides contain several bands: the most intense band is associated with the B-X transition. In the red region of the spectrum, there is a wide continuum region corresponding to $\text{C}(^2\Pi_{3/2})\text{-A}(^2\Pi_{3/2})$ transitions with maxima at 475 (XeF), 344 (XeCl), 290 (KrF), and 236 nm (KrCl). At short internuclear distances, mixing occurs between the D and B levels, lifting the interdiction against radiative transitions from the D level to the ground state. The maxima of these transitions lie in near 260 (XeF), 235.5 (XeCl), and 219 nm (KrF); the maximum of the D-X transition of KrCl was beyond the limits of the photomultiplier response. Moreover, in an Ar-Kr- NF_3 mixture, the Kr_2F band at approximately $340 \div 500 \text{ nm}$ was observed; similarly the band of Xe_2Cl ($420 \div 600 \text{ nm}$) was observed in Ar-Xe- CCl_4 , and the band of the Cl_2 ($\sim 257 \text{ nm}$) impurity was observed in Ar-Kr- CCl_4 .

For the Ar-Xe- CCl_4 mixture, the coefficient of the transformation of nuclear energy into radiation in the 308 nm band (η) was measured. The value of η was determined by comparing the estimated radiation intensity for the mixture of interest with that of the $\text{C}^3\Pi_u\text{-B}^3\Pi_g$ nitrogen band in an Ar- N_2 mixture. For an Ar (150 kPa) + Xe (5.3 kPa) + CCl_4 (93 Pa) mixture, the value of the coefficient of the transformation of the α -particle energy into emission was obtained for the band at 308 nm: $\eta = 11 \pm 3\%$. The slight difference between this value and the quantum efficiency (15%) appears to be attributable to the quenching of the B state of XeCl by CCl_4 molecules. The intensities of the KrF and KrCl bands were found to be negligible compared with the intensities of the B-X transitions of XeCl and XeF; such finding prompted more detailed research into mixtures containing xenon. The coefficient of the transformation of nuclear energy into radiation in the 351 and 353 nm bands in an ^3He (200 kPa) + Xe (4 kPa) + NF_3 (2.7 kPa) mixture was estimated, taking into account the estimated energy deposition by α particles, and a value of $\eta \sim 4\%$ was found; this value is 3 times lower than that determined for the XeCl band at 308 nm.

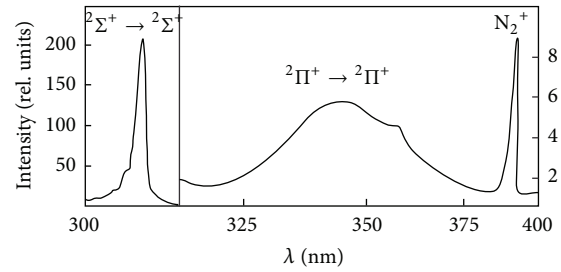


FIGURE 10: The emission spectrum of a mixture of $^3\text{He}:\text{Xe}:\text{CCl}_4 = 1500:50:1$ at $\Phi = 10^{13} \text{ n/cm}^2\text{s}$.

The B-X transition of the XeCl molecule is of the greatest interest for the creation of an excimer laser with direct nuclear pumping [76]. The high radiation resistance of the active mixture of an XeCl laser in the radiation field of a nuclear reactor was demonstrated in [16, 60]. The luminescence spectrum of an $^3\text{He}\text{-Xe-CCl}_4$ mixture under excitation by products of the $^3\text{He}(\text{n,p})^3\text{H}$ nuclear reaction in the core of a stationary nuclear reactor (Figure 10) is similar to the luminescence spectrum under excitation by α particles. In the plasma of the gas mixture, CCl_4 decays through the attachment of electrons: $\text{CCl}_4 + e \rightarrow \text{CCl}_3 + \text{Cl}^-$. For an $^3\text{He}:\text{Xe}:\text{CCl}_4 = 1500:50:1$ mixture at atmospheric pressure under a thermal-neutron flux of $10^{13} \text{ n/cm}^2\text{s}$, the rate of this decay process is $\approx 2 \cdot 10^{16} \text{ cm}^{-3} \text{ s}^{-1}$. Nevertheless, the radiation intensity in the band at 308 nm was found to remain constant at integrated neutron fluxes of up to 10^{17} n/cm^2 . This result may be related to both the presence of sufficiently fast backward processes and the formation of other chlorine compounds. The densities of ions and electrons in $^3\text{He}\text{-Xe-CCl}_4$ and $^3\text{He}\text{-Xe-}\text{NF}_3$ mixtures in the radiation field of a nuclear reactor are determined by the volt-ampere characteristics of the stationary, non-self-maintained discharge [77].

6. Conclusions

The mechanisms of level population in gas lasers pumped by ionizing radiation at the 3p-3s transitions of neon, the d-p transitions of inert gases, and the mercury triplet lines were analysed. It was shown that the dissociative recombination of molecular ions with electrons is not the basic process underlying the population of the p levels of inert-gas atoms. It is assumed that the most likely channel for d-level population is the direct excitation of atoms by secondary electrons and the excitation transfer from buffer gas atoms; in addition, the p levels are populated through transitions from the upper levels. The dissociative recombination of molecular ions with electrons is the basic process underlying the population of the 7^3S_1 level of mercury atoms and the 6^3S_1 level of cadmium atoms. The possibility of creating an efficient quasi-CW laser with ionized pumping based on the first negative system of CO was considered. The results of research concerning the emission of heteronuclear ionic molecules of inert gases and halogenides of inert gases under nuclear pumping were described.

Conflict of Interests

The author declares that there is no conflict of interests regarding the publication of this paper.

Acknowledgments

The author is grateful to E. G. Batyrbekov, A. M. Nazarov, A. B. Tleuzhanov, and N. I. Khismatullina for their assistance in conducting the experiments and to A. M. Soroka for fruitful discussions of the results.

References

- [1] R. T. Shneider and F. Hohl, "Nuclear pumped lasers," in *Advances in Nuclear Science and Technology*, J. Lewis and M. Becker, Eds., vol. 16, pp. 123–287, Plenum Press, New York, NY, USA, 1984.
- [2] S. P. Mel'nikov, A. N. Sizov, and A. A. Sinyanskii, *Nuclear Pumped Lasers*, VNIIEF, Sarov, Russia, 2008 (Russian).
- [3] A. V. Karelin, A. A. Sinyanskii, and S. I. Yakovlenko, "Nuclear-pumped lasers and physical problems in constructing a reactor-laser," *Quantum Electronics*, vol. 27, no. 5, pp. 375–402, 1997.
- [4] A. V. Zagidulin, A. V. Bochkov, V. V. Mironenko, and G. S. Sofienko, "A 500-J nuclear-pumped gas laser," *Technical Physics Letters*, vol. 38, no. 23, pp. 1059–1062, 2012.
- [5] M. U. Khasenov, *Nuclear-Induced Plasmas of Gas Mixtures and Nuclear Pumped Lasers*, Almaty, 2011 (Russian).
- [6] A. M. Voinov, L. E. Dovbysh, V. N. Krivonosov et al., "Low-threshold nuclear-pumped lasers using transitions of atomic xenon," *Soviet Physics Doklady*, vol. 24, no. 3, pp. 189–190, 1979.
- [7] B. D. Carter, M. J. Rowe, and R. T. Schneider, "Nuclear-pumped cw lasing of the $^3\text{He-Ne}$ system," *Applied Physics Letters*, vol. 36, no. 2, pp. 115–117, 1980.
- [8] G. A. Batyrbekov, M. U. Khasenov, A. B. Tleuzhanov et al., "Investigation of the active media of lasers operating in the nuclear reactor," Final Scientific Report GR 81032078, Institute of Nuclear Physics, Almaty, Kazakhstan, 1986 (Russian).
- [9] A. B. Dmitriev, V. S. Il'yashenko, A. I. Mis'kevich, and B. S. Salamakha, "Luminescence of neon and some of its mixtures at high pressures," *Optics and Spectroscopy*, vol. 43, no. 6, pp. 1165–1168, 1977.
- [10] G. A. Batyrbekov, E. G. Batyrbekov, V. A. Danilychev, and M. U. Khasenov, "Efficiency of populating neon 3p-levels under ionized pumping," *Optics and Spectroscopy*, vol. 68, no. 6, pp. 1241–1245, 1990.
- [11] O. Svelto, *Principles of Lasers*, Springer, 4th edition, 1998.
- [12] A. V. Fedenev and V. F. Tarasenko, "Simulation of NPL in experiments with e-beam pumping," *Laser and Particle Beams*, vol. 16, no. 2, pp. 327–380, 1998.
- [13] A. Ulrich, "Light emission from the particle beam induced plasma: an overview," *Laser and Particle Beams*, vol. 30, no. 2, pp. 199–205, 2012.
- [14] M. U. Khasenov, "Emission of the heteronuclear ionic molecules (ArXe^+) at excitation by a hard ionizer," in *Atomic and Molecular Pulsed Lasers VI*, vol. 6263 of *Proceedings of SPIE*, pp. 141–148, September 2006.
- [15] M. U. Khasenov, "Emission of the $^3\text{He-Xe-Cd}$ mixture in the active zone of a nuclear reactor," *Quantum Electronics*, vol. 34, no. 12, pp. 1124–1126, 2004.
- [16] G. A. Batyrbekov, M. U. Khasenov, E. Yu. Kuzmin et al., "Radiation resistance of elements of the laser system in the core of nuclear reactor," *Izvestiya Akademii Nauk Kazachskoy SSR*, no. 6, pp. 23–26, 1986 (Russian).
- [17] M. U. Khasenov, "Nuclear-induced plasma—the source of optical emission," *NNC RK Bulletin*, no. 1, pp. 55–72, 2010 (Russian).
- [18] N. G. Basov, A. Yu. Aleksandrov, V. A. Danilychev et al., "Powerful quasi-cw laser of high pressure on p-s-transitions of Ne atom," *Quantum Electronics*, vol. 15, no. 1, p. 147, 1985.
- [19] A. V. Karelin and S. I. Yakovlenko, "Kinetic model of an He-Ne-Ar- H_2 laser pumped by hard ionising radiation," *Quantum Electronics*, vol. 25, no. 8, pp. 739–745, 1995.
- [20] K. Sakasai, T. Kakuta, and M. Nakazawa, "Numerical simulation of a nuclear pumped $^3\text{He-Ne-Ar}$ gas laser for its optimization," *Japanese Journal of Applied Physics*, vol. 37, no. 9, part 1, pp. 4806–4811, 1998.
- [21] G. A. Hebner and G. N. Hays, "Fission-fragment-excited lasing at 585.3 nm in He/Ne/Ar gas mixtures," *Applied Physics Letters*, vol. 57, no. 21, pp. 2175–2177, 1990.
- [22] Y. R. Shaban and G. H. Miley, "Practical, visible wavelength nuclear-pumped laser," *Laser and Particle Beams*, vol. 11, no. 3, pp. 559–566, 1993.
- [23] A. I. Konak, S. P. Mel'nikov, V. V. Porkhaev, and A. A. Sinyanskii, "Characteristics of nuclear-pumped lasers based on the 3p-3s transitions in the neon atom," *Quantum Electronics*, vol. 25, no. 3, pp. 209–214, 1995.
- [24] J. W. Shon, R. L. Rhoades, J. T. Verdeyen, and M. J. Kushner, "Short pulse electron beam excitation of the high-pressure atomic Ne laser," *Journal of Applied Physics*, vol. 73, no. 12, pp. 8059–8065, 1993.
- [25] M. U. Khasenov, "On the mechanism of populating 3p levels of neon under pumping by a hard ioniser," *Quantum Electronics*, vol. 41, no. 3, pp. 198–201, 2011.
- [26] A. A. Mavlyutov, A. I. Mis'kevich, and B. S. Salamakha, "Nuclear pumping of Ne- O_2 and Ar- I_2 mixtures," *Laser Physics*, vol. 3, no. 1, pp. 103–109, 1993.
- [27] I. I. Smirnova and M. U. Khasenov, "Possible use of ion-ion recombination in nuclear pumped lasers," in *Atomic and Molecular Pulsed Lasers VII*, vol. 6938 of *Proceedings of SPIE*, p. 8, Tomsk, Russia, September 2007.
- [28] E. D. Poletaev, B. Yu. Dorofeev, P. P. D'yachenko et al., "Emission characteristics of pure neon and He-Ne mixture excited by a high-pressure nuclear particles," *Technical Physics*, vol. 37, no. 1, pp. 114–121, 1992.
- [29] A. A. Abramov, V. V. Gorbunov, S. P. Melnikov et al., "Luminescence of nuclear-induced rare-gas plasmas in near infrared spectral range," in *Atomic and Molecular Pulsed Lasers VI*, vol. 6263 of *Proceedings of SPIE*, pp. 279–296, May 2006.
- [30] J. P. Apruzese, J. L. Giuliani, M. F. Wolford et al., "Optimizing the Ar-Xe infrared laser on the Naval Research Laboratory's Electra generator," *Journal of Applied Physics*, vol. 104, no. 1, Article ID 013101, 2008.
- [31] D. N. Babichev, A. V. Karelin, O. V. Simakova, and H. Tomizawa, "Optimization of a He-Ar laser with an electron-beam and nuclear pumping," *Laser Physics*, vol. 12, no. 5, pp. 835–858, 2002.
- [32] C. B. Collins and F. W. Lee, "Measurement of the rate coefficients for the bimolecular and termolecular ion-molecule reactions of Ar_2^+ with selected atomic and molecular species," *Journal of Chemical Physics*, vol. 71, no. 1, pp. 184–191, 1979.

- [33] R. J. Shul, R. Passarella, B. L. Upschulte, R. G. Keesee, and A. W. Castleman Jr., "Thermal energy reactions involving Ar^+ monomer and dimer with N_2 , H_2 , Xe, and Kr," *Journal of Chemical Physics*, vol. 86, no. 8, pp. 4446–4451, 1987.
- [34] V. V. Gorbunov, V. D. Grigor'ev, L. E. Dovbysh et al., "The luminescence spectra in the 350–875 nm range of the dense gas excited by uranium fission fragments," *Proceedings of RFNC-VNIIEF*, no. 6, pp. 148–185, 2004 (Russian).
- [35] G. B. Ramos, M. Schlamkowitz, J. Sheldon, K. A. Hardy, and J. R. Peterson, "Observation of dissociative recombination of Ne_2^+ and Ar_2^+ directly to the ground state of the product atoms," *Physical Review A*, vol. 51, no. 4, pp. 2945–2950, 1995.
- [36] A. Barrios, J. W. Sheldon, K. A. Hardy, and J. R. Peterson, "Superthermal component in an effusive beam of metastable krypton: evidence of Kr_2^+ dissociative recombination," *Physical Review Letters*, vol. 69, no. 9, pp. 1348–1351, 1992.
- [37] A. B. Dmitriev, V. S. Il'yashenko, A. I. Mis'kevich et al., "Excitation of laser transitions in gas mixtures with metal vapors by products of neutron nuclear reactions," *Technical Physics*, vol. 52, no. 11, pp. 2235–2237, 1982.
- [38] G. A. Batyrbekov, E. G. Batyrbekov, A. B. Tleuzhanov, and M. U. Khasenov, "Measurement of the coefficient of conversion of nuclear energy into luminous energy in $\text{Xe}+\text{Hg}$ and $\text{Kr}+\text{Hg}$ mixtures," *Journal of Applied Spectroscopy*, vol. 47, no. 4, pp. 1069–1072, 1987.
- [39] N. G. Basov, G. A. Batyrbekov, M. U. Khasenov et al., "Method for generation in a laser on a mercury mixture with molecular gas," Patent USSR N1322950, 1985.
- [40] G. A. Batyrbekov, V. A. Dolgikh, I. G. Rudoi, A. M. Soroka, A. B. Tleuzhanov, and M. U. Khasenov, "Luminescence of mixtures of mercury and inert gases containing molecular additives with excitation by ionizing radiation," *Journal of Applied Spectroscopy*, vol. 49, no. 5, pp. 1139–1143, 1988.
- [41] R. Johnsen and M. A. Biondi, "Charge transfer of atomic and molecular rare-gas ions with mercury atoms at thermal energy," *Journal of Chemical Physics*, vol. 73, no. 10, pp. 5045–5050, 1980.
- [42] G. A. Batyrbekov, M. U. Khasenov, A. M. Soroka et al., "Feasibility of construction of a quasi-cw laser utilizing 7s-6p transitions in mercury pumped by ionizing radiation," *Quantum Electronics*, vol. 17, no. 6, pp. 774–775, 1987.
- [43] A. V. Bochkov, V. A. Kryzhanowskii, E. P. Magda et al., "Quasi-cw lasing on the 7^3S_1 - 6^3P_2 atomic mercury transition," *Technical Physics Letters*, vol. 18, no. 7, pp. 91–93, 1992.
- [44] R. L. Rhoades and J. T. Verdeyen, "Electron beam pumping of the 546.1 nm mercury laser," *Applied Physics Letters*, vol. 60, no. 24, pp. 2951–2953, 1992.
- [45] B. M. Smirnov, "Gas laser on negative ion," *Soviet Physics Doklady*, vol. 12, pp. 242–244, 1967.
- [46] M. J. Kushner, "Nuclear-reactor pumped lasers excited by ion-ion neutralization," *Journal of Applied Physics*, vol. 54, no. 1, pp. 39–47, 1983.
- [47] G. A. Batyrbekov, M. U. Khasenov, A. M. Soroka et al., "Kinetics of excited states of Hg pumping by ionizing radiation" (Russian), Preprint of the Institute of Nuclear Physics, no. 3/87, Almaty, 1987.
- [48] D. P. Greene and J. G. Eden, " $\text{Cd}(6^3\text{S}_1 \rightarrow 5^3\text{P}_1)$ laser at 480 nm pumped by a transverse discharge," *IEEE Journal of Quantum Electronics*, vol. 19, no. 12, pp. 1739–1741, 1983.
- [49] E. P. Magda, "Analysis of experimental and theoretical research of nuclear-pumped lasers at the institute of technical physics," *Laser and Particle Beams*, vol. 11, no. 3, pp. 469–476, 1993.
- [50] S. P. Bugaev, F. G. Goryunov, D. Yu. Nagornyy et al., "UV generation by electron beam pumping of He-Cd mixture," *Optics and Spectroscopy*, vol. 65, no. 3, pp. 744–747, 1988.
- [51] N. G. Basov, A. Yu. Aleksandrov, V. A. Danilychev et al., "Efficient quasi-cw laser in the first negative system of nitrogen," *JETP Letters*, vol. 42, no. 1, pp. 39–42, 1985.
- [52] M. U. Khasenov, V. A. Dolgich, and A. M. Soroka, "Kinetics of CO first negative system excitation by ionized radiation," in *Proceedings of the Specialist Conference on "Physics of Nuclear Induced Plasmas and Problems of Nuclear Pumped Lasers"*, p. 56, Obninsk, Russia, 1992.
- [53] M. U. Khasenov, "Kinetics of CO first negative system excitation by ionized radiation," in *Atomic and Molecular Pulsed Lasers V*, vol. 5483 of *Proceedings of SPIE*, pp. 14–23, May 2004.
- [54] R. A. Waller, C. B. Collins, and A. J. Cunningham, "Stimulated emission from CO^+ pumped by charge transfer from He_2^+ in the afterglow of an e-beam discharge," *Applied Physics Letters*, vol. 27, no. 6, pp. 323–325, 1975.
- [55] W. Friedl, "Krypton-Xenon Banden," *Zeitschrift für Naturforschung B*, vol. 14, no. 9, p. 848, 1959.
- [56] E. Kugler, "Über die Lumineszenz der Edelgasgemische Ar/Xe, Kr/Xe, Ar/Kr und der Gemische Xe/ N_2 und Kr/ N_2 bei Anregung mit schnellen Elektronen," *Annalen der Physik*, vol. 14, no. 3–4, pp. 137–146, 1964.
- [57] P. Millet, A. M. Barrie, A. Birot et al., "Kinetic study of $(\text{ArKr})^+$ and $(\text{ArXe})^+$ heteronuclear ion emissions," *Journal of Physics B: Atomic and Molecular Physics*, vol. 14, no. 3, article 023, pp. 459–472, 1981.
- [58] G. A. Batyrbekov, E. G. Batyrbekov, A. B. Tleuzhanov, and M. U. Khasenov, "Molecular band in an emission spectrum of Ar-Xe," *Optics and Spectroscopy*, vol. 62, no. 1, pp. 212–214, 1987.
- [59] M. U. Khasenov, "Emission of ionic molecules $(\text{KrXe})^+$ on excitation by a hard ionizer," *Journal of Applied Spectroscopy*, vol. 72, no. 3, pp. 316–320, 2005.
- [60] M. U. Khasenov, M. T. Nakiskozhaev, A. S. Syrlybaev, and I. I. Smirnova, "Emission of inert gas halides at excitation by alpha-particles," *Atmospheric and Oceanic Optics*, vol. 22, no. 11, pp. 1057–1059, 2009.
- [61] G. N. Hays, D. A. McArthur, D. R. Neal, and J. K. Rice, "Gain measurements near 351 nm in $^3\text{He}/\text{Xe}/\text{NF}_3$ mixtures excited by fragments from the $^3\text{He}(n, p)^3\text{H}$ reaction," *Applied Physics Letters*, vol. 49, no. 7, pp. 363–365, 1986.
- [62] A. I. Mis'kevich, Guo Jinbo, and A. Yu. Dyuzhov, "Spontaneous and induced emission of XeCl^* excimer molecules under pumping of Xe- CCl_4 and Ar-Xe- CCl_4 gas mixtures with a low CCl_4 content by fast electrons and uranium fission fragments," *Quantum Electronics*, vol. 43, no. 11, pp. 1003–1008, 2013.
- [63] L. I. Virin, R. V. Dzhagatspanyan, G. V. Karachevtsev et al., *Ion-Molecular Reactions in Gases*, Nauka, Moscow, Russia, 1979 (Russian).
- [64] A. A. Radzyg and B. M. Smirnov, *Reference Book on Atomic and Molecular Physics*, Atomizdat, Moscow, Russia, 1980 (Russian).
- [65] D. L. Judge and L. C. Lee, "Electronic transition moments for the $A \rightarrow X$, $B \rightarrow X$, and $B \rightarrow A$ transitions in CO^+ and the $A \leftarrow X$ and $B \leftarrow X$ moments for the $\text{CO} \rightarrow \text{CO}^+$ systems; absolute cross sections for the absorption processes," *Journal of Chemical Physics*, vol. 57, no. 1, pp. 455–462, 1972.
- [66] C. B. Collins, "The nitrogen ion laser pumped by charge transfer," *IEEE Journal of Quantum Electronics*, vol. 20, no. 1, pp. 47–63, 1984.

- [67] M. U. Khasenov, "Kinetics of the nitrogen first negative system excitation by ionising radiation," *Quantum Electronics*, vol. 35, no. 12, pp. 1104–1106, 2005.
- [68] F. W. Lee, C. B. Collins, and R. A. Waller, "Measurement of the rate coefficients for the bimolecular and termolecular charge transfer reactions of He_2^+ with Ne, Ar, N_2 , CO, CO_2 , and CH_4 ," *Journal of Chemical Physics*, vol. 65, no. 5, pp. 1605–1615, 1976.
- [69] C. B. Collins and F. W. Lee, "Measurement of the rate coefficients for the bimolecular and termolecular ion-molecule reactions of He_2^+ with selected atomic and molecular species," *Journal of Chemical Physics*, vol. 68, no. 4, pp. 1391–1401, 1978.
- [70] V. A. Dolgich, I. G. Rudoi, A. Yu. Samarin, and A. M. Soroka, "Kinetics of inversion destruction in the laser on the first negative system of nitrogen," *Quantum Electronics*, vol. 18, no. 7, pp. 854–856, 1988.
- [71] A. Yu. Aleksandrov, V. A. Dolgich, O. M. Kerimov et al., "Effective collision lasers in the visible and UV regions of spectrum," *Izvestiya Akademii Nauk SSSR*, vol. 53, no. 8, pp. 1474–1483, 1989.
- [72] Y. Tanaka, K. Yoshino, and D. E. Freeman, "Emission spectra of heteronuclear diatomic rare gas positive ions," *Journal of Chemical Physics*, vol. 62, no. 11, pp. 4484–4496, 1974.
- [73] C. Laigle and F. Collier, "Kinetic study of $(\text{ArXe})^+$ heteronuclear ion in electron beam excited Ar-Xe mixture," *Journal of Physics B: Atomic and Molecular Physics*, vol. 16, no. 4, article 021, pp. 687–697, 1983.
- [74] M. Tsuji, M. Tanaka, and Y. Nishimura, "New emission spectra of KrXe^+ produced from Kr afterglow reactions of Xe," *Chemical Physics Letters*, vol. 262, no. 3–4, pp. 349–354, 1996.
- [75] P. Millet, A. Birot, H. Brunet, M. Espagnan, J. Galy, and Y. Salmero, "Kinetic study of the KrXe^+ heteronuclear ion emission," *Journal of Physics B: Atomic and Molecular Physics*, vol. 16, no. 8, article 013, pp. 1383–1392, 1983.
- [76] A. A. Mavlyutov and A. I. Mis'kevich, "Nuclear pumped excimer laser operating at 308 nm wavelength," *Technical Physics Letters*, vol. 22, no. 4, pp. 326–327, 1996.
- [77] G. A. Batyrbekov, M. U. Khasenov, S. A. Kostriza et al., "Feasibility of excimer lasers with ionization by radiation from a nuclear reactor," *Technical Physics Letters*, vol. 8, no. 13, pp. 789–791, 1982.

